Molecular Vision 2025; 31:380-394 <http://www.molvis.org/molvis/v31/380>
Received 6 January 2025 | Accepted 3 October 2025 | Published 5 October 2025

Hyperosmolar stress induces monocyte chemoattractant protein 1 expression in retinal pigmented epithelial arising retinal pigmented epithelial 19 cells

Moncef Ould Hamou,[1,2] Maureen Masset,[1,2] Célia Weber,[1,2] Lisa Scifo,[1,2] Sarah Libert,[1,3] Angélic Bryla,[1] Françoise Gregoire,[1] Valérie Delforge,[1] Nargis Bolaky,[1] Azine Datlibagi,[1,3] Jean-Yves Springael,[4] Jason Perret,[1] François Willermain,[2,4] Christine Delporte[1]

(The first three authors contributed equally to this work.)

[1]Laboratory of Pathophysiological and Nutritional Biochemistry, Université Libre de Bruxelles, Brussels, Belgium; [2]Department of Ophthalmology, CHU St Pierre and Brugmann, Université Libre de Bruxelles, Brussels, Belgium; [3]Department of Ophthalmology, Erasme Hospital, Hôpital Universitaire de Bruxelles, Université Libre de Bruxelles, Brussels, Belgium; [4]I.R.I.B.H.M., Université Libre de Bruxelles, Brussels, Belgium

Purpose: Diabetes is a chronic inflammatory disease that may damage the blood-retinal barrier, leading to diabetic retinopathy (DR). Blood-retinal barrier rupture may subject the retinal pigmented epithelial cells to a hyperosmolar stress (HOS), activating the transcription factor nuclear factor of activated T cells 5 (NFAT5). In addition, inflammatory cytokines, such as monocyte chemoattractant protein 1 (MCP-1/CCL2), play a crucial role in DR. The aims of our study were to determine whether HOS induces MCP-1 levels in arising retinal pigmented epithelial 19 (ARPE-19) cells and to decipher the responsible intracellular cascade involved in such stimulation.

Methods: ARPE-19 cells or ARPE-19 cells transfected with dominant negative NFAT5 plasmid or NFAT5 short hairpin RNA plasmids were preincubated or not for 1 h in the absence or presence of a protein kinase or transcription factor inhibitor and then incubated for 8 h with iso-osmolar or hyperosmolar medium in the absence or presence of inhibitor. NFAT5 reporter gene activity was quantified by luminescence. MCP-1 messenger RNA (mRNA) and protein levels were determined by quantitative real-time PCR and enzyme-linked immunosorbent assay, respectively. Biologically active MCP-1 was assessed by a calcium mobilization assay performed using Chinese hamster ovary cells expressing or not the MCP-1 receptor and apoaequorin.

Results: In response to HOS, ARPE-19 cells showed a significant increase in MCP-1 mRNA levels independent of NFAT5 activation. Moreover, the MCP-1 protein secreted by ARPE-19 in response to HOS is biologically active. The use of various inhibitors of protein kinase and transcription factors suggest that the HOS-induced increase in MCP-1 mRNA levels is dependent on a protein kinase C (PKC) and/or a MEK1/2-p38 pathway activating p53, as well as a PKC-p38-PI3K-PDK1-AKT activating hypoxia-inducible factor 1 alpha (HIF1α).

Conclusion: HOS increases the expression of MCP-1 mRNA and protein levels in ARPE-19 cells, and the secreted MCP-1 is biologically active. The HOS-induced increase of MCP-1 mRNA appears to be independent of NFAT5 activation. Despite the activation of NFAT5 upon HOS and the presence of NFAT5 binding sites in the MCP-1 gene promoter, activated NFAT5 may not be sufficient to induce MCP-1 gene transactivation in response to HOS in ARPE-19 cells. The intracellular cascade involved in the HOS-induced increase of MCP-1 mRNA in ARPE-19 cells may consist of a PKC-p38-PI3K-PDK1-AKT-HIF1α axis and/or a MEK1/2-p38-p53 axis.

Diabetes is a chronic metabolic disease, currently also considered an inflammatory disease, which affects 14% of the population in Europe [1]. Diabetic retinopathy (DR), one of many complications of diabetes, is a major cause of acquired blindness in Western countries [2]. Under physiologic conditions, the homeostasis of the retina is maintained by a blood-retinal barrier (BRB). The BRB is composed of two parts: the inner BRB, made of tight junctions between retinal capillary endothelial cells, astrocytes, pericytes, and Müller cells' endfeet, and the outer BRB, made of tight junctions between retinal pigmented epithelial (RPE) cells [3]. The BRB regulates the movements of water, ions, and solutes to maintain the homeostasis of the retina [4]. In diabetes, its rupture leads to macular edema and loss of vision [5]. Following inner BRB rupture with concomitant outer limiting membrane rupture or outer BRB rupture, RPE cells are likely to be submitted to hyperosmolar stress (HOS) by the accumulation of proteins and solutes in their vicinity [6]. The persistence of exudates in the retina after edema resorption strongly suggests that

Correspondence to: Christine Delporte, Laboratory of Pathophysiological and Nutritional Biochemistry, Université Libre de Bruxelles, 808 Route de Lennik, CP611, B-1070 Brussels, Belgium; email: christine.delporte@ulb.be

RPE cells remain continuously submitted to HOS [4,7]. In response to HOS, cells rapidly shrink and then adapt using osmoadaptive mechanisms, known as regulatory volume increase, which involves two distinct steps [8,9]. During the first step, there is a rapid (within seconds) accumulation of inorganic electrolytes in the cytoplasm, which promotes cell volume increase [8,9]. During the second step, there is a slow (within hours) activation of the nuclear factor of activated T cells 5 (NFAT5), a transcription factor formerly also called tonicity enhancer binding protein (TonEBP) or osmolar response element binding protein [10,11]. Then, NFAT5 transactivates osmoprotective genes, such as aldose reductase (AR) and sodium-dependent taurine transporter, leading to intracellular organic electrolyte accumulation [12,13] and maintenance of the restored cell volume [8,9]. Depending on the cell type, various protein kinases are involved in NFAT5 activation, including protein kinase A [14], extracellular signal-regulated kinase (ERK) [15], phosphatidylinositol 3-kinase (PI3K) [16], protein kinase B (AKT) [17], p38 mitogen-activated protein kinase (p38 MAPK) [18], c-Jun N-terminal kinase (JNK) [19], tyrosine-protein kinase Fyn [18], ataxia- telangiectasia mutated kinase [16], glycogen synthase kinase 3-beta [20], mammalian target of rapamycin [21], and focal adhesion kinase [22]. It has been shown that the arising retinal pigmented epithelial 19 (ARPE-19) cells adapt to HOS using osmoadaptive mechanisms, including p38 MAPK phosphorylation and activation of NFAT5, leading to its nuclear translocation and subsequent transactivation of osmoprotective genes, such as AR and taurine transporter [7]. These mechanisms undoubtedly contribute to the accumulation of organic osmolytes and cell volume restoration in ARPE-19 cells subjected to HOS [7].

The efficacy of intravitreal steroid administration to treat diabetic macular edema emphasizes the role of inflammation in this pathological condition [23]. Several studies have analyzed the role played by cytokines in the rupture of the BRB, including that of proinflammatory cytokine monocyte chemoattractant protein 1 (MCP-1). MCP-1, involved in monocyte and basophil chemotaxis [24,25], is produced by many cell types [26], including RPE cells [27]. MCP-1 has been implicated in diabetes [28]. Indeed, high MCP-1 levels in serum [25,29], vitreous [30] or urine [31] are associated with a greater risk of diabetic complication occurrence (retinopathy and nephropathy). Moreover, an elevated vitreous MCP-1 level is associated with diabetic macular edema [32-34]. Interestingly, in the context of osmoadaptation, MCP-1 messenger RNA (mRNA) and protein levels have been shown to be upregulated by HOS in an NFAT5-dependent manner in rat kidney epithelioid cells [35], human mesothelial cells [36] and human HeLa-modified conjunctiva-derived cells [37], likely via the transactivating activity of NFAT5 on the MCP-1 gene promoter [35]. HOS has also been shown to enhance lipopolysaccharide (LPS)–induced MCP-1 levels in RPE cells [38]. However, the sole effect of HOS on MCP-1 expression has not yet been investigated in RPE cells. Therefore, the aims of our study were to determine whether HOS induces MCP-1 levels in ARPE-19 cells and to decipher the intracellular cascades involved in MCP-1 induction, including the possible involvement of NFAT5.

METHODS

Cell culture and treatment: ARPE-19 cells were purchased from ATCC-LGC Standards (Molsheim, France) and authenticated by short tandem repeat analysis using the PowerPlex 16 HS kit (Promega, Madison, WI) according to the manufacturer's instructions (ECACC, Salisbury, UK). ARPE-19 cells were grown in Dulbecco's modified Eagle's medium/Ham's F-12 medium (Thermo Fisher Scientific, Waltham, MA), containing 10% fetal bovine serum, 100 UI/ml streptomycin/penicillin (Thermo Fisher Scientific), and 4 mM glutamine (Thermo Fisher Scientific), and passaged twice a week at confluence (Appendix 1). ARPE-19 cells or transfected ARPE-19 cells (24 h after transfection) were preincubated or not for 1 h with either 0.01% dimethyl sulfoxide (DMSO; used as control) or a protein kinase or transcription factor inhibitor diluted in DMSO (to reach a final treatment concentration of 0.01% DMSO, as in the control) and then incubated for 8 h with iso-osmolar (Iso: control medium) or hyperosmolar medium (control medium containing 25 mM, 50 mM, or 100 mM sodium chloride [Na25, Na50, Na100] or 50 mM, 100 mM, or 200 mM sucrose [Su50, Su100, Su200]) in the presence of 0.01% DMSO or inhibitor (diluted in DMSO to reach a final treatment concentration of 0.01% DMSO, as in the control). As we cannot exclude some effects of inhibitors on MCP-1 levels under Iso stimulation, we compared the Na100-induced MCP-1 mRNA levels or protein levels in the presence of inhibitors diluted in DMSO with those in the presence of DMSO.

Cell transfection and SEAP activity measurement: ARPE-19 cells, at 80% of confluence, were trypsinized, centrifuged, and then resuspended in Ingenio electroporation medium (Mirus, Madison, WI) before their transfection by electroporation using a Gene Pulser Xcell (Bio-Rad Laboratories, Hercules, CA). ARPE-19 cells were transfected with short hairpin (sh) CTN (a control plasmid producing an irrelevant short hairpin RNA interference [RNAi]), sh-NFAT5 (a mix of four different sh-RNAi plasmids designed to inhibit NFAT5; Origene, Rockville, MD), a plasmid encoding for enhanced green fluorescent protein (pEGFP) used as a control plasmid

Table 1. Characteristics of the primers.

Gene	Primer sequence (5′-3′)	Accession number	Amplicon size (bp)	Efficiency (%)
ATP5b*	AGAGGTCCCATCAAAACCAAAC AAAAGCCCAATTTTGCCACC	NM_001686.3	152	98
B2M*	AGATGAGTATGCCTGCCGTG TCATCCAATCCAAATGCGGC	NM_004048.2	120	103
HPRT1*	TGGCGTCGTGATTAGTGATG CTCGAGCAAGACGTTCAGTC	NM_000194.2	137	99
MCP-1	GGTTTGCTTGTCCAGGTGG GTGTCCCAAAGAAGCTGTGATCT	NM_002582.3	109	83
YWHAZ*	ACAAAAGACGGAAGGTGCTG TCTGCTTGTGAAGCATTGGG	NM_145690.2	141	100

* Reference genes used for geNorm normalization.

(Takara Bio [Clontech], Mountain View, CA), or DN-NFAT5 (a plasmid containing a dominant negative mutant of NFAT5 coding for a truncated NFAT5 protein inhibiting its transactivating activity, kindly provided by Dr. B. Ko, University of Hong Kong, China) [39] in the absence or presence of a control plasmid or a NFAT5 reporter plasmid (pSEAP-NFAT5; a plasmid containing two binding sites for NFAT5 regulating the transcription of the reporter gene coding for a secreted embryonic alkaline phosphatase [SEAP], a generous gift from Drs. W. Neuhofer and C. Küper, Ludwig-Maximilians Universität München, Germany) [40]. Plasmids were introduced into the cells by electroporation using an exponential decay wave pulse of 270 V and 950 µF during 15 ms in a 4-mm gap cuvette, with an efficiency of 60% to 80%. SEAP activity was quantified by luminescence using a standard curve ranging from 0 to 5 mU/ml of standard SEAP, as previously described [7].

Gene expression analysis using quantitative real-time PCR: RNA extraction from ARPE-19 cells, RNA concentration and purity, and complementary DNA (cDNA) synthesis were performed as previously described [41]. Primers were designed for real-time quantitative PCR (RT-qPCR) as previously described [41] to ensure optimal amplicon size, DNA polymerization efficiency, and amplification specificity (Table 1). Possible genomic DNA amplification by the primers was verified by performing a RT-qPCR in the presence of 2.5 ng genomic DNA. The levels of mRNA were quantified by RT-qPCR reactions performed using 2.5 ng cDNA as a template and the Power Track SYBR Green master mix (Eurogentec, Seraing, Belgium) [41]. Data were analyzed using the qPCR CFX system (Bio-Rad Laboratories) and normalized with reference genes using the qbase+ software [42]. All RT-qPCR experiments were performed in accordance with the Minimum Information for publication of Quantitative real-time PCR Experiments guidelines [43]. All nontarget negative controls were performed using molecular biology grade RNase/DNase-free water instead of cDNA.

MCP-1 enzyme-linked immunosorbent assay: MCP-1 protein level were determined on cell culture supernatant by ELISA using an Hcytomag kit (Merck Millipore, Darmstadt, Germany), according to the manufacturer's instructions, in experiments evaluating the effects of Sh-NFAT5 and DN-NFAT5 on HOS-induced MCP-1 protein levels. Results were analyzed using a Magpix system (Luminex, MV's-Hertogenbosch, The Netherlands) and Bio-Plex Manager Software (Bio-Rad Laboratories). For all other experiments, MCP-1 protein level was determined in the cell culture medium using ELISA kits (R&D Diagnostics, Minneapolis, MN).

Intracellular calcium mobilization assay: The functional responses induced by MCP-1 (secreted in the cell culture medium) were analyzed with an aequorin-based assay as previously described [44]. CHO-WTA11 cells coexpressing apoaequorin and Gα16 or CHO-WTA11 cells expressing C-C chemokine receptor type 2 (CCR2), the MCP-1 receptor, were incubated for 4 h in the dark in the presence of 5 µm coelenterazine H (Promega). Some cells in suspension (25,000 cells/well) were added to wells containing 50 µl cell culture medium collected from ARPE-19 cells incubated with ISO, Na100 and Su200 in the absence or presence of DN-NFAT5. Luminescence was measured for 30 s in an EG&G Berthold luminometer (PerkinElmer Life Sciences, Waltham, MA). A stimulation with adenosine triphosphate (25 µM) was used to normalize the recorded signals. MCP-1 concentrations were determined using nonlinear regression applied to a

sigmoidal dose-response model (GraphPad Prism, version 10.2.3; GraphPad Software, La Jolla, CA).

Statistical analyses: Statistical analyses were performed using SPSS (IBM SPSS Statistics for Windows, version 20.0; IBM, Armonk, NY) or GraphPad Prism software (version 10.2.3) and the Shapiro-Wilk test, repeated-measures analysis of variance with Sidak or Bonferroni post hoc tests, the conformity *t* test, and the paired *t* test. The tests were considered statistically significant when $p < 0.05$.

RESULTS

HOS-induced dose-dependent increase in MCP-1 mRNA in ARPE-19 cells: MCP-1 mRNA levels were determined by RT-qPCR in ARPE-19 cells incubated for 8 h in Iso medium or medium supplemented with increasing concentrations of NaCl (Na25, Na50, Na100; Figure 1A) or sucrose (Su50, Su100, Su200; causing a similar increase in osmolarity as the used NaCl concentrations; Figure 1B). Both NaCl and Su significantly increased MCP-1 mRNA levels in a dose-dependent manner. Na50 and Na100 induced a 4.4-fold ($p = 0.004$) and 16.1-fold ($p = 0.004$) increase in MCP-1 mRNA levels, respectively, compared with Iso (Figure 1A). Su100 and Su200 increased 5.7-fold ($p = 0.002$) and 9.8-fold ($p = 0.001$) MCP-1 mRNA levels, respectively, compared with Iso (Figure 1B).

HOS-induced increase in MCP-1 mRNA and protein levels is independent of NFAT5 activation in ARPE-19 cells: To assess the role of NFAT5 in the HOS-induced increase in both MCP-1 mRNA and protein levels in ARPE-19 cells, the cells were transfected with either sh-CTN plasmid (control) or sh-NFAT5 RNAi expressing plasmids. Then, the cells were treated for 8 h with Iso or Na100 before quantification of MCP-1 mRNA levels and secreted protein levels by RT-qPCR or ELISA (Figure 2A,B). In ARPE-19 transfected with sh-CTN, Na100 significantly increased both MCP-1 mRNA and secreted protein levels by about 47-fold ($p = 0.025$) and 3.9-fold ($p = 0.027$), respectively, compared with Iso (Figure 2A,B). In ARPE-19 transfected with sh-NFAT5, Na100 still significantly increased MCP-1 mRNA and protein levels by about 75-fold ($p = 0.003$) and 2.8-fold ($p = 0.01$), respectively, compared with Iso (Figure 2A,B).

To confirm these data, ARPE-19 cells were also transfected with either pEGFP (as a control) or DN-NFAT5 before their treatment for 8 h with Iso or Na100 (Figure 2C,D). In control-transfected ARPE-19 cells, Na100 significantly increased MCP-1 mRNA and secreted protein levels by about 50-fold ($p < 0.001$) and 7.1-fold ($p = 0.004$), respectively, compared with Iso. In ARPE-19 cells transfected with DN-NFAT5, Na100 significantly increased MCP-1 mRNA and secreted protein levels by about 83-fold ($p = 0.048$) and 5.4-fold ($p = 0.028$), respectively, compared with Iso.

sh-NFAT5 and DN-NFAT5 decrease the transactivation activity of NFAT5 in ARPE-19 cells: To verify the efficiency of sh-NFAT5 and DN-NFAT5 on NFAT5 transactivation inhibition, the reporter activity of SEAP indicative of NFAT5 transactivation activity was measured by luminescence in the cell culture supernatant of ARPE-19 cells cotransfected with pSEAP-NFAT5 (a reporter plasmid containing two

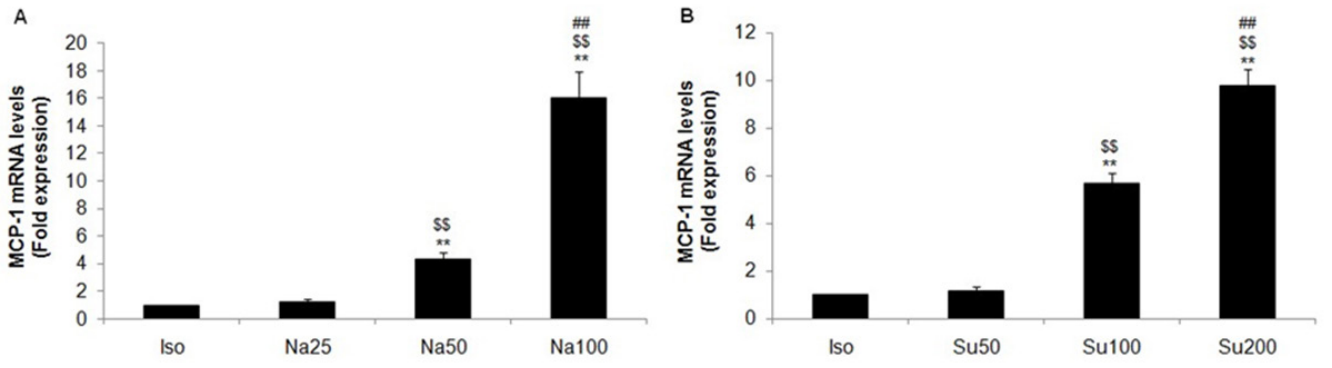

Figure 1. Hyperosmolar stress induced dose-dependent increase in MCP-1 mRNA in ARPE-19 cells. ARPE-19 cells were incubated for 8 h with iso-osmolar medium (Iso) or media containing additional increasing concentrations of NaCl (Na25, Na50, Na100; **A**) or sucrose (Su50, Su100, Su200; **B**) prior to MCP-1 mRNA levels determination by RT-qPCR, as described under Methods. Data are expressed as the mean ± SEM (n = 4) of MCP-1 mRNA levels (in fold expression) over the Iso set to 1, following normalization with appropriate reference genes (HPRT1, B2M, ATP5B). Data were analyzed using the conformity t test and the paired t test. **p < 0.01 indicates statistical significance compared to Iso; $$p < 0.01 indicates statistical significance compared to Na25 or Su50; ##p < 0.01 indicates statistical significance compared to Na50 or Su100.

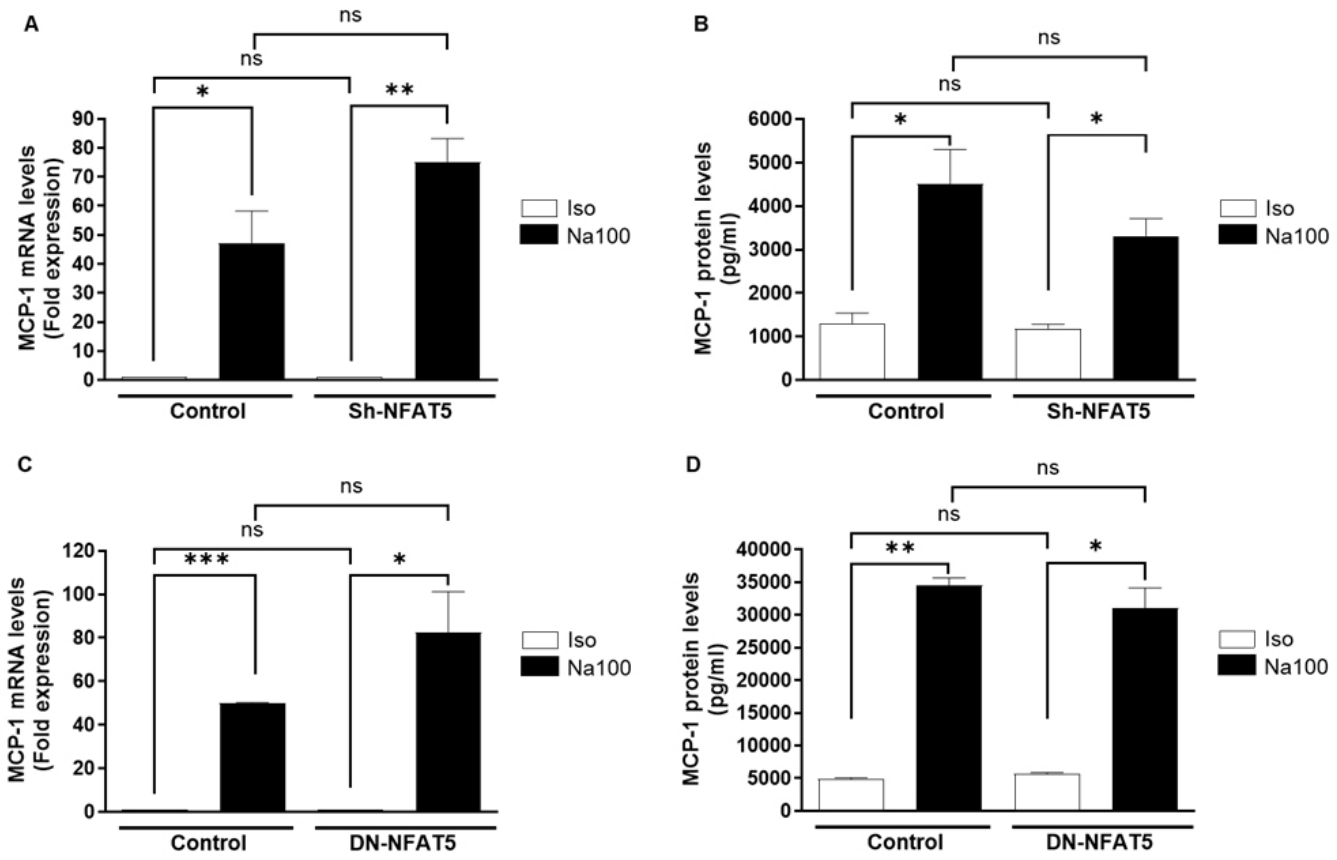

Figure 2. Hyperosmolar stress-induced increase in MCP-1 mRNA and protein is independent of NFAT5 activation in ARPE-19 cells. ARPE-19 cells were transfected with sh-CTN plasmid (control) or sh-NFAT5 plasmid (**A**, **B**); with pEGFP (control) or DN-NFAT5 plasmid (**C**, **D**), then subjected to Iso (white columns) or Na100 (black columns) for 8 h, as previously described. MCP-1 mRNA levels measured by RT-qPCR (**A**, **C**) are expressed as MCP-1 mRNA levels (in fold expression) over Iso set to 1 following normalization with appropriate reference genes (YWHAZ, B2M for sh-NFAT5 [**A**]; YWHAZ, ATP5B for DN-NFAT5 [**C**]). MCP-1 protein levels quantified by ELISA are expressed as MCP-1 protein levels (in pg/ml; B, D). Data are the mean ± SEM of four (**A**, **B**) or three (**C**, **D**) independent experiments. Data were analyzed using repeated-measures analysis of variance with Bonferroni post hoc tests, the conformity *t* test, and the paired *t* test. *$p < 0.05$, **$p < 0.01$, ***$p < 0.001$.

NFAT5 binding sites) and a control plasmid (sh-CTN plasmid [an irrelevant sh-RNAi control] or pEGFP), sh-NFAT5, or DN-NFAT5 before their treatment for 8 h with Iso or Na100 (Figure 3A,B). sh-NFAT5 and DN-NFAT5 significantly decreased by 35% ($p = 0.048$) and 86% ($p < 0.001$), respectively, Na100-induced SEAP activity (Figure 3A,B).

MCP-1 secreted by ARPE-19 cells in response to HOS is biologically active and not dependent upon NFAT5 activation: To determine the biological activity of MCP-1 produced by the ARPE-19 cells in response to HOS, the cell culture medium from cells stimulated for 24 h with Iso or Na100 was incubated with CHO-WTA11 cells expressing CCR2 (the MCP-1 receptor) [44] to measure the intracellular calcium mobilization. In the absence (control) or presence of DN-NFAT5, Na100 significantly increased the calcium mobilization levels in CHO-WAT11-CCR2 cells, with the calcium mobilization threshold set using CHO-WAT11 cells (Figure 4). However, the presence of DN-NFAT5 did not modify the calcium mobilization under Iso or Na100 compared with the corresponding conditions in the absence of DN-NFAT5 (Figure 5). With the use of a standard sigmoidal dose-response curve, the intracellular calcium increase was converted to MCP-1 concentration (Figure 5). Data indicated that in the absence of DN-NFAT5 (control), the concentration of MCP-1 in the cell culture medium was significantly higher in response to Na100 compared with Iso. In the presence of DN-NFAT5, Na100 significantly increased MCP-1 concentrations in the cell culture medium, with no significant

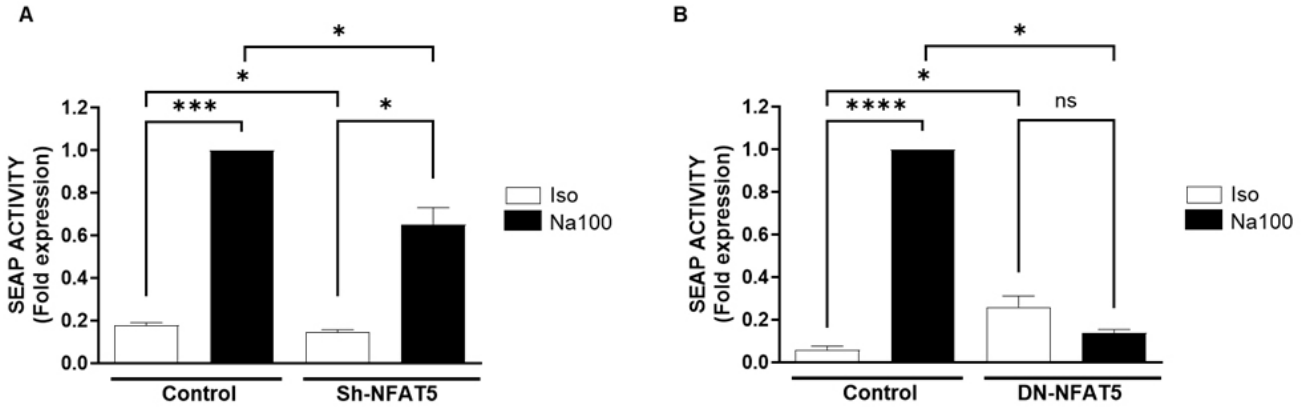

Figure 3. sh-NFAT5 and DN-NFAT5 decrease the transactivation activity of NFAT5 in ARPE-19 cells. ARPE-19 cells were transfected with pSEAP-TonE plasmid and sh-CTN (control) or sh-NFAT5 (**A**) or with pSEAP-TonE plasmid and pEGFP (control) or DN-NFAT5 (**B**). Then, ARPE-19 cells were subjected to Iso (white columns) or Na100 (black columns) for 8 h, and SEAP activity was determined as described under Methods. Data are expressed as SEAP activity (in fold over control Na100 condition set to 1) and are the mean ± SEM of three independent experiments. Data were analyzed using the conformity *t* test and the paired *t* test. *$p < 0.05$, **$p < 0.01$, ***$p < 0.001$.

difference compared with similar conditions in the absence of DN-NFAT5. These data indicate that MCP-1 secreted in the cell culture medium in response to Na100 is biologically active and that NFAT5 is not involved in HOS-driven MCP-1 expression.

HOS-induced increase in MCP-1 mRNA is dependent on p38 and PKC activation in ARPE-19 cells: The intracellular signaling cascade involved in the increase of MCP-1 mRNA levels in response to HOS was investigated using inhibitors of several protein kinases that have been previously reported in the literature to be involved in regulating MCP-1 expression. For this purpose, ARPE-19 cells were pretreated for 1 h in the absence or presence of inhibitor and then incubated for 8 h with Iso or Na100 in the absence (DMSO) or presence of inhibitor (diluted in DMSO) before MCP-1 mRNA level quantification by RT-qPCR (Figure 6A).

Among the tested inhibitors, inhibitors of PKC (GF109203X and GO6983), p38 MAPK (SB203508) and 3-phosphoinositide-dependent kinase 1 (PDK1; OSU-03012), AKT (MK-2206), PI3K (LY294002), serum and glucocorticoid-regulated kinase 1 (GSK650394), ERK1/2 (roscovitine), and MEK1/2 (UO126) significantly decreased Na100-induced MCP-1 mRNA levels (Figure 6A). Other tested inhibitors, including GO6976 (PKC), wortmannin (PI3K), EDM638683 (serum and glucocorticoid-regulated kinase 1), SP600125 (JNK), SCH772984 (ERK1/2), PD98059 (MEK1/2), rapamycin (mammalian target of rapamycin), and decernotinib (Janus kinase), did not significantly impair Na100-induced MCP-1 mRNA levels (Figure 6A).

HIF1α and p53 may be involved in MCP-1 transcription in response to HOS in ARPE-19 cells: After identifying the protein kinases that may be involved in the intracellular cascade leading to MCP-1 expression in response to HOS, we evaluated the involvement of some transcription factors that have been previously reported in the literature to be activated by these protein kinases and involved in MCP-1 transactivation. To this end, we tested different inhibitors of cyclic AMP response element-binding protein (CREB), nuclear factor–κB, specificity protein 1 (SP1), activating protein 1 (AP1), hypoxia-inducible factor 1 alpha (HIF1α), and tumor protein p53 (p53) on the Na100-induced increase in MCP-1 mRNA levels (Figure 6B).

Echinomycin (a HIF1α inhibitor) and pifithrin (a p53 inhibitor) significantly reduced the Na100-induced MCP-1 mRNA levels. However, inhibitors of CREB (666-15), nuclear factor–κB (CAPE), SP1 (mithramycin), and AP1 (SR11302) did not significantly impair Na100-induced MCP-1 mRNA levels (Figure 6B).

The involvement of PKC, p38 MAPK, HIF1α, and p53 on HOS-induced MCP-1 transcription is corroborated on secreted MCP-1 protein levels: Considering Na100-induced MCP-1 mRNA levels may involve a PKC-p38-PI3K-PDK1-AKT-HIF1α axis and/or a MEK1/2-p38-p53 axis, we focused on evaluating the effects of PKC, p38 MAPK, HIF1α, and p53 inhibitors on Na100-induced secreted MCP-1 protein levels. Our data showed that inhibitors of PKC (GF109203X), p38 MAPK (SB203580), HIF1α (echinomycin), and p53 (pifithrin) significantly reduced the secreted MCP-1 protein

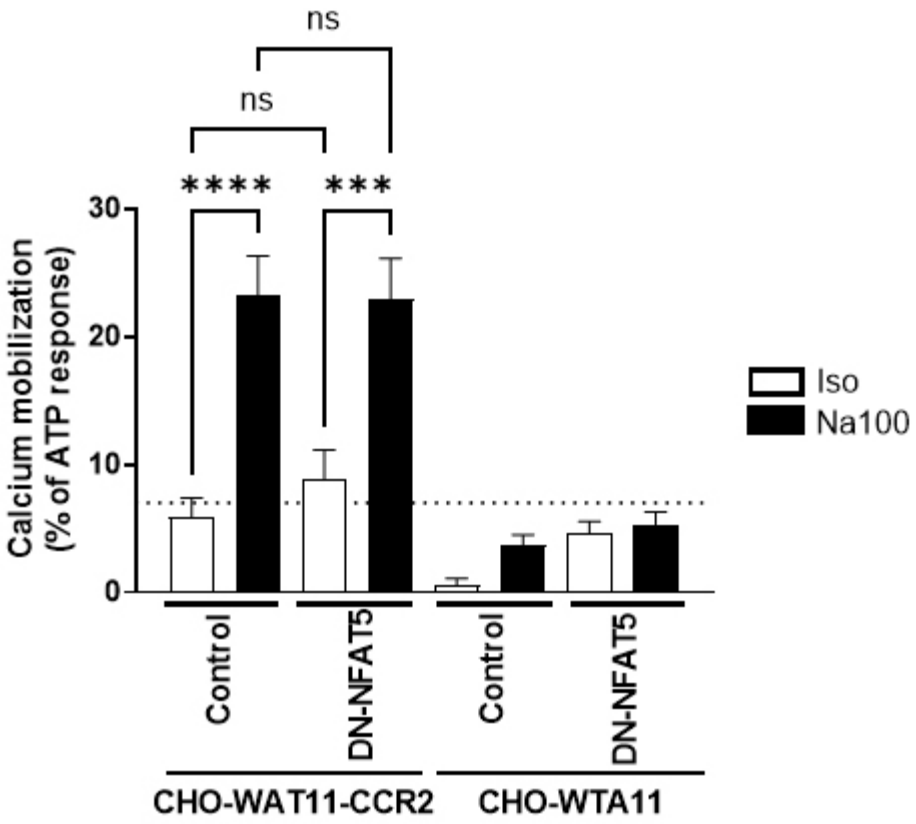

Figure 4. The MCP-1 produced by ARPE-19 cells is biologically active, as measured by the calcium mobilization assay. ARPE-19 cells transfected with an EGFP plasmid (control) or with a DN-NFAT5 plasmid were incubated for 8 h with Iso or Na100. The cell supernatants were then collected and applied to CHO-WTA11 cells expressing CCR2 to measure calcium mobilization. The results were normalized for baseline activity (0%) and the maximal response obtained with 25 µM adenosine triphosphate (100%). The dotted line indicates the calcium mobilization threshold set using CHO-WAT11 cells. The displayed data are the mean ± SEM of four independent experiments and measurements performed in duplicates. Data were analyzed using the one-way analysis of variance and post hoc Sidak's tests. *$p < 0.05$, **$p < 0.01$, ***$p < 0.001$.

levels, corroborating their effects on the MCP-1 mRNA levels (Figure 6C).

DISCUSSION

In diabetes, hyperglycemia activates metabolic pathways, leading to overexpression of proangiogenic and proinflammatory molecules such as vascular endothelial growth factor (VEGF), interleukin 6, and MCP-1. Furthermore, inflammation is involved in the genesis and maintenance of macular edema during DR, compromising the patient's visual acuity [45-48].

Macrophages recruited under the action of MCP-1 secrete various proangiogenic molecules, such as VEGF, and proinflammatory molecules, resulting in structural modification of the BRB and leukostasis in retinal capillaries, promoted in part by overproduction of intercellular adhesion molecule 1 [26,46,48,49]. It has been shown that MCP-1 expression increased in response to 20 mM and 40 mM NaCl in the presence of LPS or LPS alone [38]. However, to our knowledge, it has never been shown that HOS alone could induce MCP-1 in RPE or ARPE-19 cells. As the vitreous of patients with DR has abnormally high levels of MCP-1 [50-52], we postulated that HOS consequent to BRB rupture [53] induces an abnormal secretion of MCP-1 by the RPE. We showed for the first time a dose-dependent increase in MCP-1 mRNA levels in response to hyperosmolar concentrations of NaCl and Su in ARPE-19 cells. These data are in concordance with a previous study showing a dose-dependent increase in MCP-1 mRNA levels in response to HOS in rat kidney epithelioid cells [35]. Moreover, by studying calcium mobilization concomitant to MCP-1 binding to its receptor, we showed that the MCP-1 secreted by ARPE-19 cells in response to HOS was biologically active. Therefore, during DR, MCP-1 may be released upon RPE exposure to HOS, thereby contributing to macrophage recruitment and disease development.

Considering the central role of NFAT5 in the tissue response to osmotic stress [54], including ARPE-19 cells [53], we first investigated its role in HOS-induced MCP-1 induction. Our results clearly showed that neither sh-NFAT5 nor DN-NFAT5 reduced HOS-induced MCP-1 mRNA or protein levels, despite their ability to decrease or suppress the NFAT5 transactivation activity. sh-NFAT5 reduced

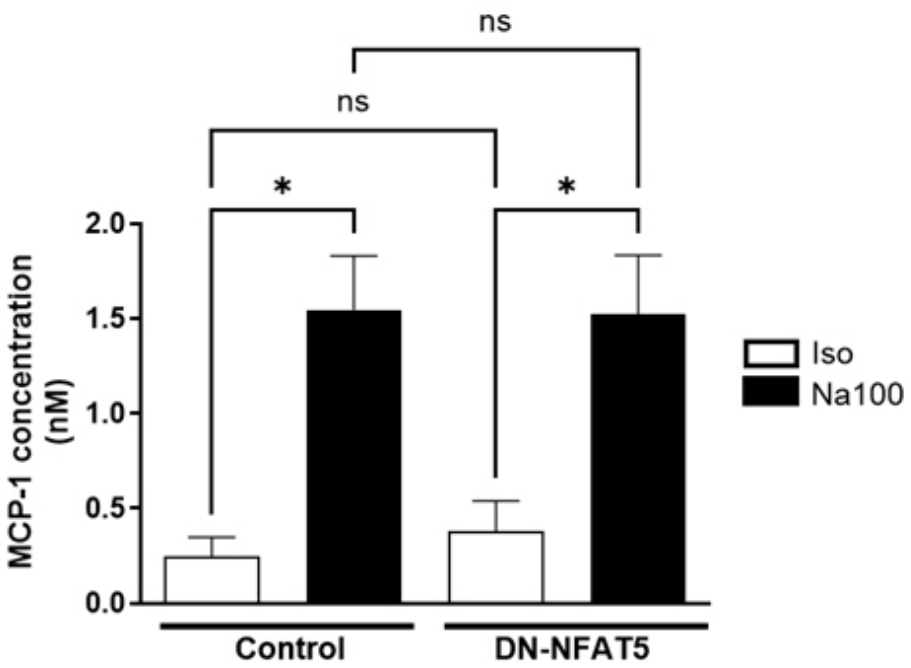

Figure 5. DN-NFAT5 does not affect MCP-1 concentration in the cell culture medium of ARPE-19 cells incubated with Na100. ARPE-19 cells transfected with an EGFP plasmid (control) or with DN-NFAT5 plasmid were incubated for 8 h with Iso or Na100. The cell supernatants were then collected and applied to CHO-WTA11 cells expressing CCR2 to measure calcium mobilization. The results were normalized for baseline activity (0%) and the maximal response obtained with 25 µM adenosine triphosphate (100%). MCP-1 concentration was then determined using a standard curve. MCP-1 concentration (nM) is the mean ± SEM of four independent experiments and measurements performed in duplicates. Data were analyzed using the one-way analysis of variance and post hoc Sidak's tests. *$p < 0.05$, **$p < 0.01$.

HOS-induced SEAP activity to a lower extent (35% reduction) than DN-NFAT5 (86% reduction). This could result from the low efficacy of sh-NFAT5 to decrease NFAT5 mRNA (31% reduction; Appendix 2) and/or the increased half-life of NFAT5 mRNA in response to HOS (>24 h) compared with the isosmotic condition (±6 h) in response to 100 mM NaCl [7]. The higher efficiency of DN-NFAT5 is likely related to its direct binding to NFAT5, thereby blocking its transactivating activity using the reporter plasmid pSEAP-NFAT5. Furthermore, we deliberately chose not to use NFAT5 inhibitors: KRN2 (13-[(2-Fluorophenyl)methyl]-5,6-dihydro-9,10-dimethoxy-benzo[g]-1,3-benzodioxolo[5,6-a]quinolizinium chloride) or KRN5 (13-(2-fluorobenzyl)-9,10-dimethoxy-5,6-dihydro-8H- [1,3]dioxolo[4,5-g]isoquinolino[3,2-a] isoquinolin-8-one). These inhibitors act on NFAT5 indirectly, whereas DN- NFAT5 and shNFAT5 act directly on NFAT5 protein and mRNA, respectively. Therefore, our data suggest that NFAT5 activation was not involved in HOS-driven transcription of MCP-1, in contrast with data obtained in other studies on different cell types. Indeed, in mesothelial cells and in human HeLa-modified conjunctiva-derived cells, the HOS-induced increase in both MCP-1 mRNA and protein expression was significantly inhibited using small interfering RNA targeting NFAT5 [36,37]. In rat kidney epithelial cells, the HOS-induced increase in MCP-1 expression may result from the binding of activated NFAT5 to an NFAT5 binding site, known as the TonE site, identified in the MCP-1 gene promoter [35]. However, HOS can induce some effects independently of NFAT5, such as the production of several proteins like heparin-binding epidermal growth factor-like growth factor [55], aquaporin 8 [56], and the inward-rectifier potassium channel 2 [57] in RPE cells. Therefore, cell-specific signal integration is a finely tuned mechanism presumably accounting for distinct responses resulting in these different data.

To further decipher the mechanism involved in HOS-induced MCP-1 transcription, we assessed the effects of several protein kinases and transcription factors inhibitors based on literature. Despite the known limitations of inhibitors, such as their nonspecific effects, our data suggest a possible pathway with p38 MAPK as its cornerstone. p38 MAPK could be activated by MEK and then phosphorylate the transcription factor p53. p38 MAPK could also be activated by PKC and then phosphorylate HIF1α via the PI3K-PDK1-AKT axis. In turn, p53 and HIF1α could then both induce MCP-1 transcription (Figure 7).

With respect to p38, four isoforms have been described: p38α, p38β, p38γ, and p38δ [58]. In our experiments, SB203580, considered a p38α inhibitor, significantly

decreased HOS-induced MCP-1 mRNA levels. Our data agree with a study showing the involvement of p38α in HOS-induced MCP-1 expression in rat kidney cells. Interestingly, in that study, p38α-driven MCP-1 induction involved NFAT5, in contrast to what we observe in ARPE-19 cells [35]. As mentioned above, these controversial data may be explained by distinct cell-specific distinct mechanisms leading or not to the involvement of NFAT5 in the regulation of MCP-1 transcription.

Various intracellular pathways have been identified to participate in the pathophysiology of DR, notably PKC activation [2]. PKC can activate p38 [35] and phosphorylate several transcription factors capable of transactivating MCP-1. Our data suggest that PKC, which can be present in several isoforms, may be involved in the transcriptional regulation of HOS-induced MCP-1 in ARPE-19 cells, in agreement with a study performed in rat mesothelial cells [59]. Indeed, PKC inhibitors, such as GF109203X and GO6983, decreased HOS-induced MCP-1 mRNA levels in ARPE-19 cells. It is interesting to note that GF109203X and riluzole, which are other PKC inhibitors, decreased MCP-1 mRNA and protein levels in diabetic pericytes [60]. However, GO6976, another PKC inhibitor, did not impact HOS-induced MCP-1 mRNA levels in ARPE-19 cells. This apparent discordance of results may be explained by the specificities of PKC inhibitors toward the 'conventional' isoforms, dependent on diacylglycerol (DAG) and intracellular calcium (Ca2+; α, β and γ), 'novel' isoforms, dependent on DAG but not Ca2+ (δ, ε, η), and 'atypical' isoforms, independent on DAG and Ca2+ (ζ) [61]. Considering that ARPE-19 cells do not express γ and η isoforms [62], it is possible that α, β, δ, ε, and ζ isoforms may be involved in the intracellular signaling pathway leading to MCP-1 expression in response to HOS. In addition, since GO6983 (the sole PKC inhibitor tested that can inhibit PKCζ) decreases HOS-induced MCP-1 mRNA levels, PKCζ may be involved in the HOS-induced MCP-1 response, as previously reported in an inflammatory "ischemia-reperfusion" model in rat retinal cells [63]. It has been shown that alternative splicing

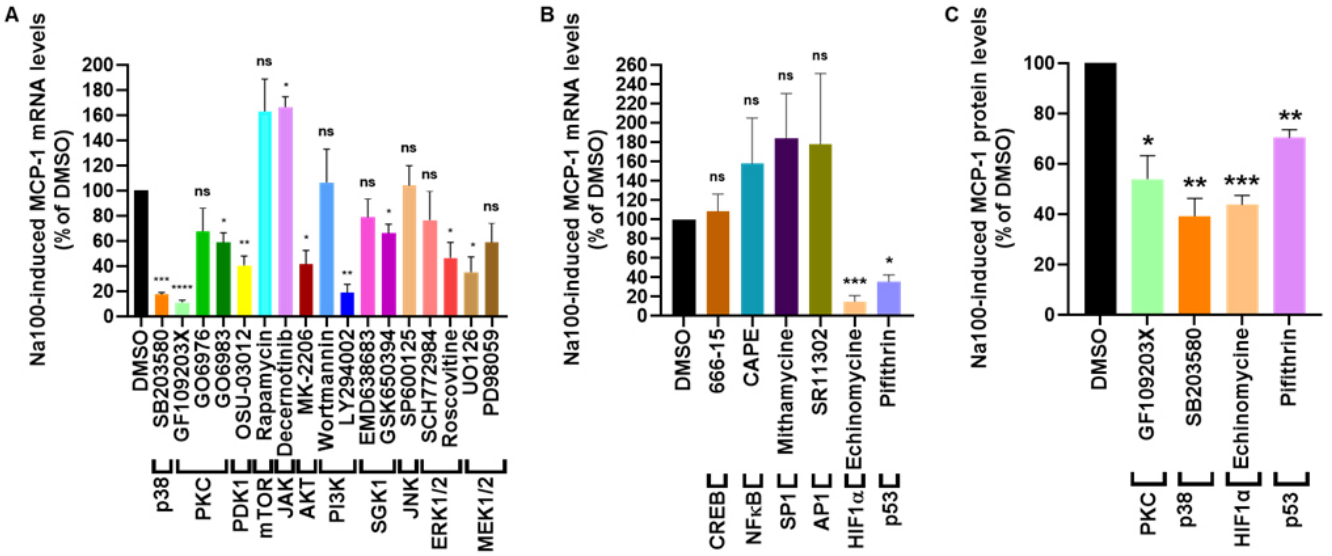

Figure 6. Protein kinase and transcription factor inhibitors affect Na100-induced MCP-1 mRNA levels. ARPE-19 cells were pretreated for 1 h with 0.01% DMSO or inhibitor diluted in DMSO (to reach a final treatment concentration of 0.01% DMSO) and then incubated for 8 h with Iso or Na100 in the presence of 0.01% DMSO or inhibitor diluted in DMSO (to reach a final treatment concentration of 0.01% DMSO) prior to quantification of MCP-1 mRNA levels by RT-qPCR (**A**, **B**) or secreted MCP-1 protein levels by ELISA (**C**), as described under Methods. The inhibitors were used at the following concentrations: 1 µM SB203580, 2.5 µM GF109203X, 1 µM GO6976, 1 µM GO6983, 10 µM OSU-03012, 0.1 µM rapamycin, 1 µM decernotinib, 1 µM SCH772984, 10 µM MK-2206, 0.1 µM wortmannin, 50 µM LY294002, 10 µM EMD638683, 10 µM GSK650394, 50 µM SP600125, 2 µM roscovitine, 5 µM UO126, 20 µM PD98059, 0.25 µM 666-15, 5 µM CAPE, 0.25 µM mithramycin, 5 µM SR11302, 0.5 µM echinomycin, or 10 µM pifithrin. Data are expressed as the mean ± SEM of the percentage of Na100-induced MCP-1 mRNA levels (A, B) or secreted MCP-1 protein levels (C) in the presence of DMSO, set as 100%; n = 3 for rapamycin, decernotinib, pifithrin, SCH772984, and SB253580 and n = 4 for all other inhibitors and DMSO (**A**, **B**, **C**). Data were analyzed using the conformity t test. *p < 0.05, **p < 0.01, ***p < 0.001.

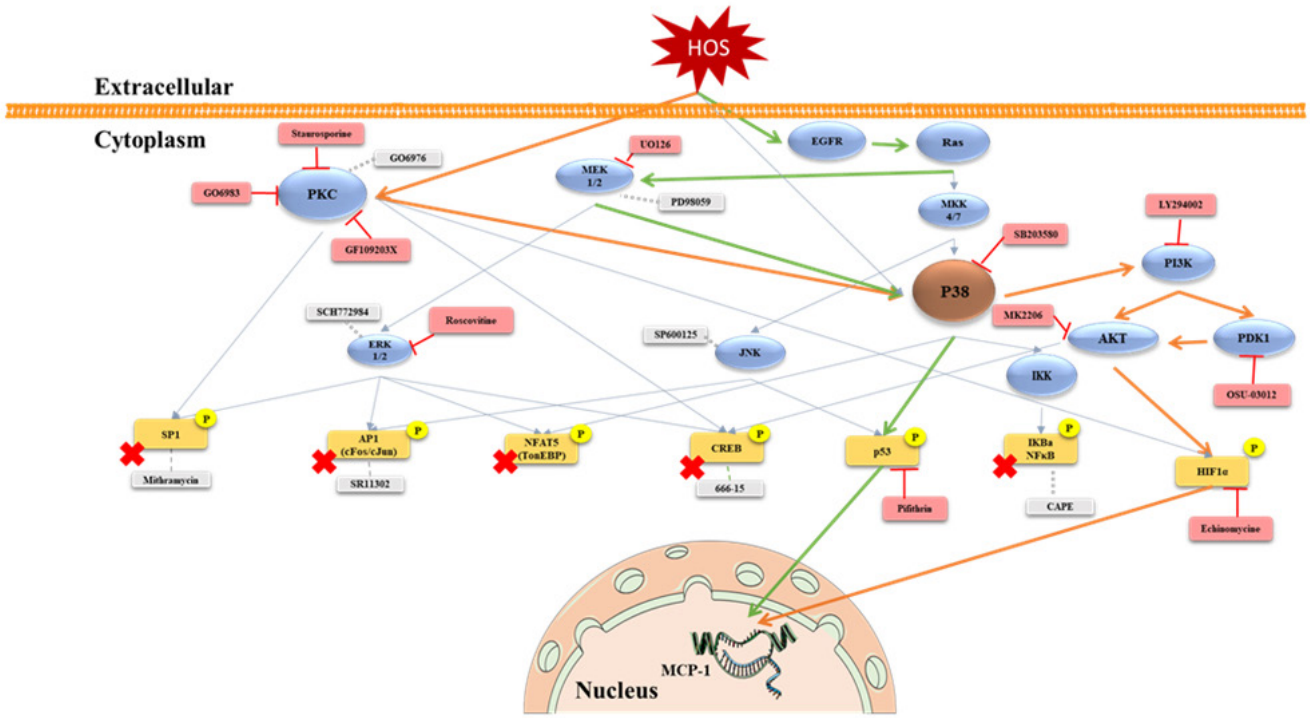

Figure 7. Some intracellular signaling pathways are potentially involved in MCP-1 transactivation in response to HOS in ARPE-19 cells. We suggest a possible pathway with p38 MAPK as its cornerstone, with p38 MAPK that can be either activated by MEK and then phosphorylate the transcription factor p53 (green arrows), or activated by PKC and then phosphorylate HIF1α via the PI3K-PDK1-AKT axis (orange arrows). p53 and HIF1α could therefore both induce MCP-1 transcription.

of PKCβ mRNA generates two versions of the protein: PKCβ1 and PKCβ2 [64]. The involvement of PKCβ2 in DR has been suggested by the improvement of retinal circulation in diabetic rats following administration of a specific inhibitor of PKCβ1/2, ruboxistaurin [65]. In addition, a randomized double-blind study shows that ruboxistaurin reduces vision loss in patients with moderate to severe nonproliferative DR [66]. In addition, GF109203X and riluzole, used for the treatment of amyotrophic lateral sclerosis and inhibiting PKCβ, decrease the mRNA and protein levels of MCP-1 in diabetic pericytes [60].

Consequently, the distinct effects of three PKC inhibitors (GF109203X, GO6976, and GO6983) tested on the HOS-induced MCP-1 mRNA level in ARPE-19 cells may be related to their variable effect on PKC isoforms or nonspecific effects of PKC inhibitors on other proteins further down the signaling cascade. For example, GF109203X may induce a decrease in MCP-1 mRNA levels by an off-target effect on AKT [67], as AKT inhibition by a specific inhibitor (MK-2206) also appears to reduce HOS-driven MCP-1 mRNA levels.

Considering our results, PKC seems to be involved in the intracellular signaling pathway, inducing MCP-1 expression in response to HOS in ARPE-19 cells. However, further targeted experiments should be performed to identify the PKC isoform(s) involved in the process.

Downstream of the PKC-p38 axis, our data highlight a possible axis implicating PI3K-PDK1-AKT and HIF1α that may lead to HOS-induced MCP-1 expression. We showed that HOS-induced MCP-1 mRNA levels were reduced by a PI3K inhibitor (LY294002), as well as by an inhibitor of PDK1 (OSU-03012). Considering PI3K and PDK1 can phosphorylate AKT, we tested the effects of an AKT inhibitor (MK-2206) and found that it also decreased HOS-induced MCP-1 mRNA levels. Our hypothesis is supported by a study showing that p38 MAPK and AKT phosphorylation are significantly increased by high NaCl concentrations in ARPE-19 cells [38]. In addition, we showed that an inhibitor of HIF1α (echinomycin) markedly decreased the levels of MCP-1 mRNA induced by HOS in ARPE-19 cells. HIF1α is a ubiquitous transcription factor stabilized in response to hypoxia but also to other stimuli, including HOS in human RPE cells [68], as well as by AKT signaling [69]. Moreover, HIF1α may transactivate MCP-1 during a pulmonary allergic inflammatory response [70] and can induce VEGF in response to HOS in

human RPE cells following the activation of p38 MAPK and PI3K [68]. Therefore, the PKC-p38-PI3K-PDK1-AKT-HIF1α axis may participate in HOS-induced MCP-1 expression in ARPE-19 cells. However, additional studies are needed to confirm this hypothesis. The involvement of GSK1 in the signaling cascade is unlikely. Indeed, the significant decrease of HOS-induced MCP-1 mRNA levels by GSK650394, but not EMD638683, may be due to its lower specificity related to nonspecific inhibition of other kinases [71].

Based on our data, another pathway may also participate in the HOS-induced increase in MCP-1 mRNA levels. This pathway may involve the activation of p38 MAPK by MEK1/2, followed by the phosphorylation of p53, which in turn may activate the transcription of MCP-1. This hypothesis is supported by data showing that a high concentration of glucose and mannitol increased the phosphorylation of MEK1/2, ERK1/2, p38 MAPK, JNK, and PKC in rat mesothelial cells [59]. In addition, it was suggested that MEK1/2 phosphorylates ERK1/2, p38 MAPK, and JNK in response to high concentrations of NaCl in cultured mouse medullary cells [72]. Furthermore, our data indicated that UO126, a MEK1/2 inhibitor, and roscovitine, an ERK1/2 inhibitor, both decreased HOS-induced MCP-1 mRNA levels in ARPE-19 cells. However, the inhibitors PD98059, SCH772984, and SP600125, acting on MEK1/2, ERK1/2, and JNK, respectively, did not impair HOS-induced MCP-1 mRNA levels in ARPE-19 cells. The different affinities of PD98059 and UO126 for MEK could explain these inconsistent results, considering UO126 has a 100-fold higher affinity than PD98059 for MEK1/2. In addition, PD98059, at the concentration used (20 μM), may have nonspecific effects. On the other hand, other transcription factors can be phosphorylated by ERK1/2 and bind to the MCP-1 gene promoter, such as AP1, SP1, CREB, and p53. High concentrations of glucose stimulate MCP-1 expression in peritoneal mesothelial cells by activating AP1 [35], while CREB is thought to participate in MCP-1 expression in response to IL-1β in ARPE-19 cells [73]. Our data show that SR11302, an AP1 inhibitor, does not affect HOS-induced MCP-1 expression in ARPE-19 cells, consistent with data obtained in kidney cells [35]. In addition, inhibitors of SP1 (mithramycin) and CREB (666-15) did not affect the HOS-induced MCP-1 mRNA levels in ARPE-19 cells. These results suggest that AP1, SP1, and CREB may not be involved in HOS-induced transactivation of MCP-1 in ARPE-19 cells. Nevertheless, a p53 inhibitor, pifithrin, reduced the levels of MCP-1 mRNA induced by HOS in ARPE-19 cells. In addition, p53 can transactivate MCP-1 and be phosphorylated by p38 or JNK [74]. However, a JNK inhibitor, SP600125, did not decrease HOS-induced MCP-1 mRNA levels, suggesting that p38 may activate p53 and thus transactivate MCP-1. However, further detailed studies would be required to validate this possibility.

In conclusion, our results show that HOS increases the expression of MCP-1 mRNA and protein levels in ARPE-19 cells and that the secreted MCP-1 is biologically active. In addition, the HOS-induced increase of MCP-1 mRNA appears to be independent of NFAT5 activation. Despite the activation of NFAT5 upon HOS and the presence of NFAT5 binding sites in the MCP-1 gene promoter, activated NFAT5 may not be sufficient to induce MCP-1 gene transactivation in response to HOS in ARPE-19 cells. The intracellular cascade involved in the HOS-induced increase of MCP-1 mRNA in ARPE-19 cells may consist of a PKC-p38-PI3K-PDK1-AKT-HIF1α axis and/or a MEK1/2-p38-p53 axis (Figure 7). As such, phosphoproteomic studies may prove valuable in further deciphering the intracellular signaling pathway involved in HOS-induced MCP-1 gene transactivation and test our hypothesis. At any rate, data suggest HOS plays a dichotomous role by activating inflammatory and osmoprotective responses in RPE cells. Considering the relatively undifferentiated state of ARPE-19 cells, further studies using fully differentiated human RPE cells derived from primary culture or embryonic or induced pluripotent stem cells may be required to confirm the data obtained from ARPE-19 cells. In addition, further studies will also be warranted to study the involvement of MCP-1 in DR in vivo. Rodents have been shown to display similarities to humans but cannot be used to study all ocular pathologies associated with diabetes due to the lack of macula, making these models unsuitable for understanding diabetic macula edema, a common complication of DR [30]. Nevertheless, the availability of knockout mice makes them desirable and useful to study the involvement of a particular gene in DR. In such respect, streptozotocin-induced DR in MCP-1 knockout mice would allow deciphering the role of MCP-1 in DR in vivo. These prospects could lead to innovative new treatments and enable specific targeting of MCP-1. This could pave the way for a new approach to diabetic macular edema refractory to current treatments and give millions of people a chance to see better.

APPENDIX 1. STR ANALYSIS.

To access the data, click or select the words "Appendix 1."

APPENDIX 2. SUPPLEMENTAL FIGURE 1.

To access the data, click or select the words "Appendix 2." Hyperosmolar stress-induced increase in NFAT5 mRNA is reduced by sh-NFAT5. ARPE-19 cells were transfected with Sh-CTN plasmid (Control) or Sh-NFAT5 plasmid; then subjected to Iso (white columns) or Na100 (black columns)

for 8h as described previously. NFAT5 mRNA levels are expressed in fold expression over Iso set to 1 following normalization with appropriate reference genes. Data are the mean ± S.E.M. of 6 independent experiments. Data were analyzed using the conformity t-test and the paired t-test. *: p<0.05, **: p<0.01 and ***: p<0.001.

ACKNOWLEDGMENTS

The authors thank Françoise Mascart, Violette Dirix and Anne Van Praet for providing assistance with Multiplex analysis. Figure 6 was partly generated using Servier Medical Art, provided by Servier, licensed under a Creative Commons Attribution 3.0 Unported license (https://creativecommons.org/licenses/by/3.0/). This work was supported by grants from the Foundation Brugmann (Brussels, Belgium; to L.S., C.W., F.W.) and the André Vésale Association (Brussels, Belgium; to M.O.H., M.M., L.S.), and the Funds for Research in Ophthalmology (FRO; Brussels, Belgium; to S.L.). Author Contributions: Conceived and design the research: C.D., F.W., J.P.; Conducted experiments resulting in the data: M.O.H., M.M., C.W., L.S., S.L., A.B., A.D., F.G., V.D., N.B., J.Y.S.; Analyzed and interpreted the data: M.O.H., M.M., C.W., L.S., S.L., A.B., F.G., J.Y.S., J.P., F.W., C.D.; Obtained the funding: M.O.H., M.M., C.W., L.S., S.L., C.D. and F.W.; Supervised research personnel: C.D., F.W., J.P.; Drafted the manuscript: C.D., M.O.H., M.M., C.W.; Made critical revision of the manuscript for important intellectual content: C.D., J.Y.S., M.O.H, A.D, J.P. and F.W. All authors have read and agreed to the published version of the manuscript. The data presented in this study are available upon request from the corresponding author. The authors declare no conflict of interest.

REFERENCES

1. . NCD Risk Factor Collaboration (NCD-RisC). Worldwide trends in diabetes prevalence and treatment from 1990 to 2022: a pooled analysis of 1108 population-representative studies with 141 million participants. Lancet 2024; 404:2077-93. [PMID: 39549716].
2. Fong DS, Aiello L, Gardner TW, King GL, Blankenship G, Cavallerano JD, Ferris FL 3rd, Klein R. American Diabetes Association. Retinopathy in diabetes. Diabetes Care 2004; 27:Suppl 1S84-7. [PMID: 14693935].
3. Kaur C, Foulds WS, Ling EA. Blood-retinal barrier in hypoxic ischaemic conditions: basic concepts, clinical features and management. Prog Retin Eye Res 2008; 27:622-47. [PMID: 18940262].
4. Strauss O. The retinal pigment epithelium in visual function. Physiol Rev 2005; 85:845-81. [PMID: 15987797].
5. Vinores SA, Gadegbeku C, Campochiaro PA, Green WR. Immunohistochemical localization of blood-retinal barrier breakdown in human diabetics. Am J Pathol 1989; 134:231-5. [PMID: 2916645].
6. Willermain F, Libert S, Motulsky E, Salik D, Caspers L, Perret J, Delporte C. Origins and consequences of hyperosmolar stress in retinal pigmented epithelial cells. Front Physiol 2014; 5:199-[PMID: 24910616].
7. Libert S, Willermain F, Weber C, Bryla A, Salik D, Gregoire F, Bolaky N, Caspers L, Perret J, Delporte C. Involvement of TonEBP/NFAT5 in osmoadaptative response of human retinal pigmented epithelial cells to hyperosmolar stress. Mol Vis 2016; 22:100-15. [PMID: 26912969].
8. Hoffmann EK, Pedersen SF. Cell volume homeostatic mechanisms: effectors and signalling pathways. Acta Physiol (Oxf) 2011; 202:465-85. [PMID: 20874806].
9. Burg MB, Ferraris JD, Dmitrieva NI. Cellular response to hyperosmotic stresses. Physiol Rev 2007; 87:1441-74. [PMID: 17928589].
10. Ho SN. The role of NFAT5/TonEBP in establishing an optimal intracellular environment. Arch Biochem Biophys 2003; 413:151-7. [PMID: 12729611].
11. Miyakawa H, Woo SK, Dahl SC, Handler JS, Kwon HM. Tonicity-responsive enhancer binding protein, a rel-like protein that stimulates transcription in response to hypertonicity. Proc Natl Acad Sci U S A 1999; 96:2538-42. [PMID: 10051678].
12. Cheung CY, Ko BC. NFAT5 in cellular adaptation to hypertonic stress - regulations and functional significance. J Mol Signal 2013; 8:5-[PMID: 23618372].
13. Lee SD, Choi SY, Lim SW, Lamitina ST, Ho SN, Go WY, Kwon HM. TonEBP stimulates multiple cellular pathways for adaptation to hypertonic stress: organic osmolyte-dependent and -independent pathways. Am J Physiol Renal Physiol 2011; 300:F707-15. [PMID: 21209002].
14. Ferraris JD, Persaud P, Williams CK, Chen Y, Burg MB. cAMP-independent role of PKA in tonicity-induced transactivation of tonicity-responsive enhancer/ osmotic response element-binding protein. Proc Natl Acad Sci U S A 2002; 99:16800-5. [PMID: 12482947].
15. Tsai TT, Guttapalli A, Agrawal A, Albert TJ, Shapiro IM, Risbud MV. MEK/ERK signaling controls osmoregulation of nucleus pulposus cells of the intervertebral disc by transactivation of TonEBP/OREBP. J Bone Miner Res 2007; 22:965-74. [PMID: 17371162].
16. Irarrazabal CE, Burg MB, Ward SG, Ferraris JD. Phosphatidylinositol 3-kinase mediates activation of ATM by high NaCl and by ionizing radiation: Role in osmoprotective transcriptional regulation. Proc Natl Acad Sci U S A 2006; 103:8882-7. [PMID: 16728507].
17. Roth I, Leroy V, Kwon HM, Martin PY, Féraille E, Hasler U. Osmoprotective transcription factor NFAT5/TonEBP modulates nuclear factor-kappaB activity. Mol Biol Cell 2010; 21:3459-74. [PMID: 20685965].
18. Ko BCB, Lam AKM, Kapus A, Fan L, Chung SK, Chung SSM. Fyn and p38 signaling are both required for maximal

hypertonic activation of the osmotic response element-binding protein/tonicity-responsive enhancer-binding protein (OREBP/TonEBP). J Biol Chem 2002; 277:46085-92. [PMID: 12359721].

19. Küper C, Beck FX, Neuhofer W. NFAT5-mediated expression of S100A4 contributes to proliferation and migration of renal carcinoma cells. Front Physiol 2014; 5:293-[PMID: 25152734].

20. Zhou X, Wang H, Burg MB, Ferraris JD. Inhibitory phosphorylation of GSK-3β by AKT, PKA, and PI3K contributes to high NaCl-induced activation of the transcription factor NFAT5 (TonEBP/OREBP). Am J Physiol Renal Physiol 2013; 304:F908-17. [PMID: 23324178].

21. Ortells MC, Morancho B, Drews-Elger K, Viollet B, Laderoute KR, López-Rodríguez C, Aramburu J. Transcriptional regulation of gene expression during osmotic stress responses by the mammalian target of rapamycin. Nucleic Acids Res 2012; 40:4368-84. [PMID: 22287635].

22. Neuhofer W, Küper C, Lichtnekert J, Holzapfel K, Rupanagudi KV, Fraek ML, Bartels H, Beck FX. Focal adhesion kinase regulates the activity of the osmosensitive transcription factor TonEBP/NFAT5 under hypertonic conditions. Front Physiol 2014; 5:123-[PMID: 24772088].

23. Elman MJ, Aiello LP, Beck RW, Bressler NM, Bressler SB, Edwards AR, Ferris FL 3rd, Friedman SM, Glassman AR, Miller KM, Scott IU, Stockdale CR, Sun JK. Diabetic Retinopathy Clinical Research Network. Randomized trial evaluating ranibizumab plus prompt or deferred laser or triamcinolone plus prompt laser for diabetic macular edema. Ophthalmology 2010; 117:1064-1077.e35. [PMID: 20427088].

24. Jiang Y, Beller DI, Frendl G, Graves DT. Monocyte chemoattractant protein-1 regulates adhesion molecule expression and cytokine production in human monocytes. J Immunol 1992; 148:2423-8. [PMID: 1348518].

25. Guan R, Purohit S, Wang H, Bode B, Reed JC, Steed RD, Anderson SW, Steed L, Hopkins D, Xia C, She JX. Chemokine (C-C motif) ligand 2 (CCL2) in sera of patients with type 1 diabetes and diabetic complications. PLoS One 2011; 6:e17822[PMID: 21532752].

26. Deshmane SL, Kremlev S, Amini S, Sawaya BE. Monocyte chemoattractant protein-1 (MCP-1): an overview. J Interferon Cytokine Res 2009; 29:313-26. [PMID: 19441883].

27. Holtkamp GM, Kijlstra A, Peek R, de Vos AF. Retinal pigment epithelium-immune system interactions: cytokine production and cytokine-induced changes. Prog Retin Eye Res 2001; 20:29-48. [PMID: 11070367].

28. Wang W, He M, Huang W. Association of monocyte chemoattractant protein-1 gene 2518A/G polymorphism with diabetic retinopathy in type 2 diabetes mellitus: A meta-analysis. Diabetes Res Clin Pract 2016; 120:40-6. [PMID: 27505625].

29. Jiang Z, Hennein L, Xu Y, Bao N, Coh P, Tao L. Elevated serum monocyte chemoattractant protein-1 levels and its genetic polymorphism is associated with diabetic retinopathy in Chinese patients with Type 2 diabetes. Diabet Med 2016; 33:84-90. [PMID: 25981750].

30. Yoshida S, Kubo Y, Kobayashi Y, Zhou Y, Nakama T, Yamaguchi M, Tachibana T, Ishikawa K, Arita R, Nakao S, Sassa Y, Oshima Y, Kono T, Ishibashi T. Increased vitreous concentrations of MCP-1 and IL-6 after vitrectomy in patients with proliferative diabetic retinopathy: possible association with postoperative macular oedema. Br J Ophthalmol 2015; 99:960-6. [PMID: 25631486].

31. Shoukry A, Bdeer Sel-A, El-Sokkary RH. Urinary monocyte chemoattractant protein-1 and vitamin D-binding protein as biomarkers for early detection of diabetic nephropathy in type 2 diabetes mellitus. Mol Cell Biochem 2015; 408:25-35. [PMID: 26104579].

32. Funk M, Schmidinger G, Maar N, Bolz M, Benesch T, Zlabinger GJ, Schmidt-Erfurth UM. Angiogenic and inflammatory markers in the intraocular fluid of eyes with diabetic macular edema and influence of therapy with bevacizumab. Retina 2010; 30:1412-9. [PMID: 20711086].

33. Owen LA, Hartnett ME. Soluble mediators of diabetic macular edema: the diagnostic role of aqueous VEGF and cytokine levels in diabetic macular edema. Curr Diab Rep 2013; 13:476-80. [PMID: 23649946].

34. Noma H, Mimura T, Yasuda K, Shimura M. Role of inflammation in diabetic macular edema. Ophthalmologica 2014; 232:127-35. [PMID: 25342084].

35. Kojima R, Taniguchi H, Tsuzuki A, Nakamura K, Sakakura Y, Ito M. Hypertonicity-induced expression of monocyte chemoattractant protein-1 through a novel cis-acting element and MAPK signaling pathways. J Immunol 2010; 184:5253-62. [PMID: 20368270].

36. Küper C, Beck FX, Neuhofer W. NFAT5 contributes to osmolality-induced MCP-1 expression in mesothelial cells. Mediators Inflamm 2012; 2012:513015[PMID: 22619484].

37. Warcoin E, Baudouin C, Gard C, Brignole-Baudouin F. In Vitro Inhibition of NFAT5-Mediated Induction of CCL2 in Hyperosmotic Conditions by Cyclosporine and Dexamethasone on Human HeLa-Modified Conjunctiva-Derived Cells. PLoS One 2016; 11:e0159983[PMID: 27486749].

38. Zhang D, Wang C, Cao S, Ye Z, Deng B, Kijlstra A, Yang P. High-Salt Enhances the Inflammatory Response by Retina Pigment Epithelium Cells following Lipopolysaccharide Stimulation. Mediators Inflamm 2015; 2015:197521[PMID: 26783382].

39. Ko BCB, Turck CW, Lee KWY, Yang Y, Chung SSM. Purification, identification, and characterization of an osmotic response element binding protein. Biochem Biophys Res Commun 2000; 270:52-61. [PMID: 10733904].

40. Neuhofer W, Steinert D, Fraek ML, Beck FX. Prostaglandin E2 stimulates expression of osmoprotective genes in MDCK cells and promotes survival under hypertonic conditions. J Physiol 2007; 583:287-97. [PMID: 17556390].

41. Arsenijevic T, Grégoire F, Delforge V, Delporte C, Perret J. Murine 3T3-L1 adipocyte cell differentiation model: validated reference genes for qPCR gene expression analysis. PLoS One 2012; 7:e37517[PMID: 22629413].

42. Vandesompele J, De Preter K, Pattyn F, Poppe B, Van Roy N, De Paepe A, Speleman F. Accurate normalization of real-time quantitative RT-PCR data by geometric averaging of multiple internal control genes. Genome Biol 2002; 3:RESEARCH0034[PMID: 12184808].

43. Bustin SA, Benes V, Garson JA, Hellemans J, Huggett J, Kubista M, Mueller R, Nolan T, Pfaffl MW, Shipley GL, Vandesompele J, Wittwer CT. The MIQE guidelines: minimum information for publication of quantitative real-time PCR experiments. Clin Chem 2009; 55:611-22. [PMID: 19246619].

44. Corbisier J, Galès C, Huszagh A, Parmentier M, Springael JY. Biased signaling at chemokine receptors. J Biol Chem 2015; 290:9542-54. [PMID: 25614627].

45. Tan GS, Cheung N, Simó R, Cheung GCM, Wong TY. Diabetic macular oedema. Lancet Diabetes Endocrinol 2017; 5:143-55. [PMID: 27496796].

46. Rübsam A, Parikh S, Fort PE. Role of Inflammation in Diabetic Retinopathy. Int J Mol Sci 2018; 19:942-[PMID: 29565290].

47. Jo DH, Yun JH, Cho CS, Kim JH, Kim JH, Cho CH. Interaction between microglia and retinal pigment epithelial cells determines the integrity of outer blood-retinal barrier in diabetic retinopathy. Glia 2019; 67:321-31. [PMID: 30444022].

48. Semeraro F, Cancarini A, dell'Omo R, Rezzola S, Romano MR, Costagliola C. Diabetic Retinopathy: Vascular and Inflammatory Disease. J Diabetes Res 2015; 2015:582060[PMID: 26137497].

49. Altmann C, Schmidt MHH. The Role of Microglia in Diabetic Retinopathy: Inflammation, Microvasculature Defects and Neurodegeneration. Int J Mol Sci 2018; 19:110-[PMID: 29301251].

50. Noma H, Mimura T, Yasuda K, Motohashi R, Kotake O, Shimura M. Aqueous Humor Levels of Soluble Vascular Endothelial Growth Factor Receptor and Inflammatory Factors in Diabetic Macular Edema. Ophthalmologica 2017; 238:81-8. [PMID: 28564655].

51. Cheung CMG, Vania M, Ang M, Chee SP, Li J. Comparison of aqueous humor cytokine and chemokine levels in diabetic patients with and without retinopathy. Mol Vis 2012; 18:830-7. [PMID: 22511846].

52. Wu J, Zhong Y, Yue S, Yang K, Zhang G, Chen L, Liu L. Aqueous Humor Mediator and Cytokine Aberrations in Diabetic Retinopathy and Diabetic Macular Edema: A Systematic Review and Meta-Analysis. Dis Markers 2019; 2019:6928524[PMID: 31871502].

53. Willermain F, Scifo L, Weber C, Caspers L, Perret J, Delporte C. Potential Interplay between Hyperosmolarity and Inflammation on Retinal Pigmented Epithelium in Pathogenesis of Diabetic Retinopathy. Int J Mol Sci 2018; 19:1056-[PMID: 29614818].

54. Go WY, Liu X, Roti MA, Liu F, Ho SN. NFAT5/TonEBP mutant mice define osmotic stress as a critical feature of the lymphoid microenvironment. Proc Natl Acad Sci U S A 2004; 101:10673-8. [PMID: 15247420].

55. Veltmann M, Hollborn M, Reichenbach A, Wiedemann P, Kohen L, Bringmann A. Osmotic Induction of Angiogenic Growth Factor Expression in Human Retinal Pigment Epithelial Cells. PLoS One 2016; 11:e0147312[PMID: 26800359].

56. Schnabel B, Kuhrt H, Wiedemann P, Bringmann A, Hollborn M. Osmotic regulation of aquaporin-8 expression in retinal pigment epithelial cells in vitro: Dependence on K_{ATP} channel activation. Mol Vis 2020; 26:797-817. [PMID: 33456300].

57. Klose E, Kuhrt H, Kohen L, Wiedemann P, Bringmann A, Hollborn M. Hypoxic and osmotic expression of Kir2.1 potassium channels in retinal pigment epithelial cells: Contribution to vascular endothelial growth factor expression. Exp Eye Res 2021; 211:108741[PMID: 34425102].

58. Jiang Y, Gram H, Zhao M, New L, Gu J, Feng L, Di Padova F, Ulevitch RJ, Han J. Characterization of the structure and function of the fourth member of p38 group mitogen-activated protein kinases, p38δ. J Biol Chem 1997; 272:30122-8. [PMID: 9374491].

59. Matsuo H, Tamura M, Kabashima N, Serino R, Tokunaga M, Shibata T, Matsumoto M, Aijima M, Oikawa S, Anai H, Nakashima Y. Prednisolone inhibits hyperosmolarity-induced expression of MCP-1 via NF-kappaB in peritoneal mesothelial cells. Kidney Int 2006; 69:736-46. [PMID: 16518329].

60. Choi JA, Chung YR, Byun HR, Park H, Koh JY, Yoon YH. The anti-ALS drug riluzole attenuates pericyte loss in the diabetic retinopathy of streptozotocin-treated mice. Toxicol Appl Pharmacol 2017; 315:80-9. [PMID: 27939241].

61. Ringvold HC, Khalil RA. Protein Kinase C as Regulator of Vascular Smooth Muscle Function and Potential Target in Vascular Disorders. Adv Pharmacol 2017; 78:203-301. [PMID: 28212798].

62. Tenconi PE, Giusto NM, Salvador GA, Mateos MV. Phospholipase D1 modulates protein kinase C-epsilon in retinal pigment epithelium cells during inflammatory response. Int J Biochem Cell Biol 2016; 81:Pt A67-75. [PMID: 27793751].

63. Lin CM, Titchenell PM, Keil JM, Garcia-Ocaña A, Bolinger MT, Abcouwer SF, Antonetti DA. Inhibition of Atypical Protein Kinase C Reduces Inflammation-Induced Retinal Vascular Permeability. Am J Pathol 2018; 188:2392-405. [PMID: 30220554].

64. Aiello LP. The potential role of PKC beta in diabetic retinopathy and macular edema. Surv Ophthalmol 2002; 47:Suppl 2S263-9. [PMID: 12507628].

65. Ishii H, Jirousek MR, Koya D, Takagi C, Xia P, Clermont A, Bursell SE, Kern TS, Ballas LM, Heath WF, Stramm LE, Feener EP, King GL. Amelioration of vascular dysfunctions in diabetic rats by an oral PKC beta inhibitor. Science 1996; 272:728-31. [PMID: 8614835].

66. Lang GE. Treatment of diabetic retinopathy with protein kinase C subtype Beta inhibitor. Dev Ophthalmol 2007; 39:157-65. [PMID: 17245085].

67. Anastassiadis T, Deacon SW, Devarajan K, Ma H, Peterson JR. Comprehensive assay of kinase catalytic activity reveals features of kinase inhibitor selectivity. Nat Biotechnol 2011; 29:1039-45. [PMID: 22037377].

68. Hollborn M, Vogler S, Reichenbach A, Wiedemann P, Bringmann A, Kohen L. Regulation of the hyperosmotic induction of aquaporin 5 and VEGF in retinal pigment epithelial cells: involvement of NFAT5. Mol Vis 2015; 21:360-77. [PMID: 25878490].

69. Toschi A, Lee E, Gadir N, Ohh M, Foster DA. Differential dependence of hypoxia-inducible factors 1 α and 2 α on mTORC1 and mTORC2. J Biol Chem 2008; 283:34495-9. [PMID: 18945681].

70. Baay-Guzman GJ, Bebenek IG, Zeidler M, Hernandez-Pando R, Vega MI, Garcia-Zepeda EA, Antonio-Andres G, Bonavida B, Riedl M, Kleerup E, Tashkin DP, Hankinson O, Huerta-Yepez S. HIF-1 expression is associated with CCL2 chemokine expression in airway inflammatory cells: implications in allergic airway inflammation. Respir Res 2012; 13:60-[PMID: 22823210].

71. Sherk AB, Frigo DE, Schnackenberg CG, Bray JD, Laping NJ, Trizna W, Hammond M, Patterson JR, Thompson SK, Kazmin D, Norris JD, McDonnell DP. Development of a small-molecule serum- and glucocorticoid-regulated kinase-1 antagonist and its evaluation as a prostate cancer therapeutic. Cancer Res 2008; 68:7475-83. [PMID: 18794135].

72. Umenishi F, Schrier RW. Hypertonicity-induced aquaporin-1 (AQP1) expression is mediated by the activation of MAPK pathways and hypertonicity-responsive element in the AQP1 gene. J Biol Chem 2003; 278:15765-70. [PMID: 12600999].

73. Cheng SC, Huang WC, S Pang JH, Wu YH, Cheng CY. Quercetin Inhibits the Production of IL-1β-Induced Inflammatory Cytokines and Chemokines in ARPE-19 Cells via the MAPK and NF-κB Signaling Pathways. Int J Mol Sci 2019; 20:2957-[PMID: 31212975].

74. Hacke K, Rincon-Orozco B, Buchwalter G, Siehler SY, Wasylyk B, Wiesmüller L, Rösl F. Regulation of MCP-1 chemokine transcription by p53. Mol Cancer 2010; 9:82-[PMID: 20406462].

Articles are provided courtesy of Emory University and The Abraham J. & Phyllis Katz Foundation. The print version of this article was created on 5 October 2025. This reflects all typographical corrections and errata to the article through that date. Details of any changes may be found in the online version of the article.